# A quantitative analysis of single protein–ligand complex separation with the atomic force microscope

Bruce E. Shapiro, Hong Qian *

*Department of Biomathematics, School of Medicine, University of California at Los Angeles, Los Angeles, CA 90095-1766, USA*

## Abstract

Force measurements on and within single macromolecular complexes utilizing techniques such as atomic force microscopy, optical trapping, flexible glass fibers, and magnetic beads provide a rich source of quantitative data on biomolecular processes. Stochastic thermal fluctuations, an undesirable source of noise in macroscopic biochemical experiments, are an essential element of these sensitive and novel experiments. With the proper analysis, a great deal of information can be gleaned from measurements of these fluctuations. A quantitative framework for analyzing such measurements, based on Kramers' theory of molecular dissociation, is developed. The analysis reveals the kinetic origin and stochastic nature of the measurements. This framework is presented in the context of protein–ligand separation with the atomic force microscope. © 1997 Elsevier Science B.V.

*Keywords:* Bond rupture; Dissociation kinetics; Kramers' rate theory; Molecular mechanics; Nano-biochemistry; Thermal fluctuation

## 1. Introduction

The state of the art for studying biological macromolecular interactions in aqueous solution has reached a stage where the behavior of the molecules and molecular complexes themselves can be individually observed. Studies of single biomolecules have already provided a rich source of information on their behavior, interactions, and the mechanisms by which they operate, as testified by the pioneer studies on single channel proteins in membranes [1,2]. At the single-molecule level, the inevitable thermal fluctuations in the measurements are no longer an unde-

sirable source of noise but are rather an integral and valuable part of the experimental data. The process of obtaining information in these delicate experiments frequently requires stochastic analysis of seemingly random results from repeated experimental measurements [3,4].

Several techniques have been developed in recent years to measure the force involved in interactions between individual macromolecules or within single macromolecular complexes [5–8]. In a set of recent experiments, the atomic force microscope (AFM) has been put to novel use in studying the bonding force within a single protein–ligand complex [9,10] or between complementary strands of DNA [11,12]. The force required to rupture the bond between the ligand and the protein has been measured directly in these experiments. The AFM probe, or cantilever, is

* Corresponding author. Address for correspondence: Department of Applied Mathematics, 408 Guggenheim Hall, University of Washington, Seattle, WA 98195-2420, USA.
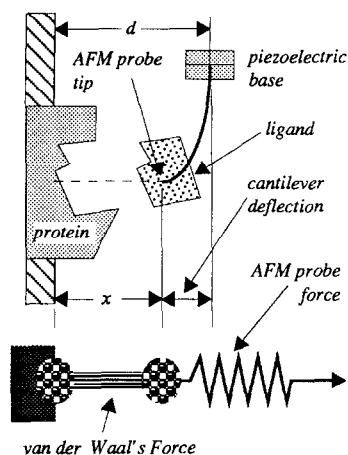
Fig. 1. Top: schematic overview of protein–ligand complex separation with the AFM. Bottom: one-dimensional model.

attached to the ligand and exerts a disruptive force upon the bond, while the protein is held fixed (Fig. 1). The base of the probe is controlled by a piezoelectric motor which increases the force exerted on the ligand by moving the probe away from the substrate, until the bond is broken. In each measurement, the positions of both the tip and the base of the probe are recorded. Once calibrated, the distance between the tip and the base measures the external force being exerted on the molecule. Usually the probe can be treated as a Hookean spring with a simple harmonic potential. The harmonic potential-well and the intermolecular interaction constitute a double-well potential in which protein–ligand dissociation takes place.

The force exerted when the bond is broken — the jumping-off force of the microscope — is sometimes naively interpreted as the 'bond rupture force'. However, the protein–ligand dissociation forced by the AFM occurs in a stochastic fashion due to the thermal motion of the pair in solution. A unique, measurable quantity which can be defined as a 'bond rupture force' does not exist. In any single experiment, the bond may break at any point over a range of forces which are a function of the probe velocity. With this realization, we have developed a quantitative framework for interpreting this type of experimental measurement based on Kramers' rate theory of molecular dissociation [13]. This framework also applies to various other molecular force measure-

ments, such as those with optical trapping [5,6], reflection interference microscopy [14,15] flexible glass fibers [7], and magnetic beads [8].

## 2. Theory

Measurements which probe molecular interactions must exert external forces on the molecular complex. The total force on the ligand is the sum of the probe and intermolecular forces. The total potential energy is:

$$E(x) = U_{intermolecular}(x) + U_{probe}(x) \qquad (1)$$

Classically, the ligand is thought to sit at an equilibrium position, measured with respect to the protein, where the total force is zero. At this point the intermolecular and probe forces are exactly balanced. This constitutes an equilibrium measurement, in which the force being exerted on the probe is recorded. As we will show, if the probe is rigid enough then the equilibrium position is unique and controllable. However, if the stiffness of the probe and the intermolecular potential are on the same order of magnitude, then a wide range of interesting dynamic phenomena occur. Our basic assumption is that the probe (the AFM tip) introduces a harmonic potential to the one-dimensional protein–ligand complex. Thus, the total potential energy is

$$E(x) = U(x) + \frac{k}{2}(x - d)^2 \qquad (2)$$

where the protein is fixed on the substrate ($x = 0$), the ligand is at a position $x$, and $U(x)$ is the intermolecular potential. The minimum force required to separate the ligand from the protein, or disruptive force, is immediately derivable from two parameters which are controlled by the experimenter: $d$, the position of piezoelectric motor, and $k$, the Hookean constant of the AFM cantilever. The total force on the ligand at $x$ is $-dE(x)/dx$.

In order to present our analysis quantitatively, we assume that the intermolecular force can be expressed as a van der Waals' potential

$$U(x) = -V_0\left[2\left(\frac{x_0}{x}\right)^6 - \left(\frac{x_0}{x}\right)^{12}\right] \qquad (3)$$

where $x$ is the intermolecular separation, $x_0$ is the equilibrium separation, and $V_0$ is the magnitude of the energy well depth [16]. The true intermolecular potential will be more complicated than this simple van der Waals' form, especially in the presence of complicated protein conformations which include multiple binding contacts [17]. Applying a similar analysis to other intermolecular potentials is computationally straightforward. Since many potential functions can be phenomenologically fit by Eq. (3), it is reasonable to use the van der Waals' model as a first order approximation. Our fundamental result will be developed from Kramers' theory of molecular dissociation (see Eq. (9)), which depends only on the curvatures of the reactant well and activation barrier. As will be described below, the curvatures are fit with a lowest order Taylor expansion about equilibrium as harmonic forces. While the results may quantitatively differ with other force models, their qualitative form should be unchanged.

At the equilibrium position of $E(x)$ the force exerted on the ligand by the protein is equal to the force on the AFM tip, for any given value of $d$. Therefore the intermolecular force as a function of $x$, $F = -\partial U/\partial x = k(x - d)$ can be obtained by slowly changing $d$. For a certain range of values of $d$ there are two stable equilibriums, a molecular well and a harmonic well (Fig. 2). Outside this range of $d$-values, one of the wells will disappear.

Rupture may occur over a wide range of probe forces (Fig. 2). We define the minimum rupture force and the critical rupture force, respectively, as the force which is exerted on the probe when $E(x)$ switches from one-well to two-well and from two-well to one-well. Because of thermal fluctuation, a single macromolecular complex may rupture anywhere between the minimum and critical rupture forces. Hence there is no unique value which can be determined experimentally corresponding to the 'rupture force'. If one is willing to wait long enough, a transition between the two wells will always occur. As the cantilever is moved away from the sample, the height of the potential barrier which must be crossed lowers, and the rate of escape increases. As one moves the cantilever faster, the mean measured rupture force is closer to the critical rupture force since there is less time for the thermal activated transition to occur.
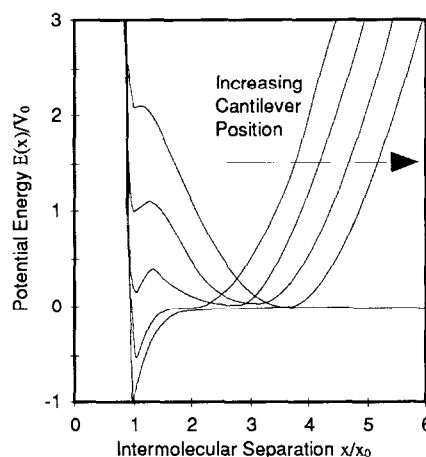


Fig. 2. Total potential energy for various positions of the controlled piezoelectric motor. Left to right: $d = 2.0$, 2.5, 3.0, 3.5 $x_0$ and the spring constant is $kx_0^2 / V_0 = 1$. The bottom curve gives the pure van der Waal's function.

When dissociation occurs, the ligand will fall to the equilibrium position of the harmonic potential. As seen from Fig. 2, the intermolecular spacing stays nearly constant while the activation barrier diminishes with increasing $d$. Furthermore, the distance between the two wells does not go to zero before the molecular well disappears. Hence there is a region for $x$ where $E(x)$ can never have a minimum for any $d$. This is a blind region for the measurement since the force in this region is not measurable. The larger the harmonic force constant $k$, the smaller the blind region. When the bending constant $k$ is greater then a critical value, i.e. the cantilever is sufficiently stiff, the potential will always have a single well. This is the traditional mode of measuring force and the full range of the intermolecular interaction can be determined.

## 2.1. The classical mechanics of protein–ligand separation and critical rupture

We will demonstrate that dissociation of a molecular complex by a Hookean spring has some interesting and unexpected behavior. Even in classical mechanics, rupture is not an inherent property of the molecular potential. At sufficiently slow speed, the dissociation process constitutes a set of equilibrium measurements, and the critical rupture force depends on the stiffness of the spring, as well as the velocity
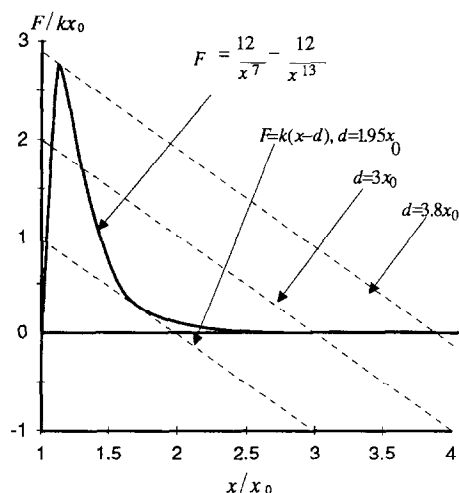
Fig. 3. Total force at various cantilever positions $d$. Solid curves: intermolecular force; dashed lines: cantilever force. $x_0$ is the equilibrium protein–ligand separation.

of the probe. Furthermore, the total energy required to rupture the bond is also a function of probe stiffness, even for the equilibrium measurement (see below). Hence it is not without error to estimate the bond energy from the energy involved in rupturing the bond.

There is an important conceptual difference between the bonding force measurement and bond rupture force measurement using the AFM. As we have stated, the equilibrium force measurement is made when the probe is stiff enough so that the total potential has a single equilibrium point at all time. The phenomenon of bond rupture, on the other hand, is inherently a feature of the double-well, one in which the ligand is held just prior to the rupture, and a second well in which the ligand is held just after rupture. This intricate balance of forces between the intermolecular bond and the AFM cantilever is illustrated in Fig. 3, where we plot the intermolecular and probe forces instead of energies, as a function of protein–ligand separation [18]. The set of parallel lines represents the force exerted on the ligand by the AFM tip for different cantilever positions $d$. Their slopes are the tip stiffness $k$. Increasing the stiffness of the probe makes these lines steeper (not shown). The ligand is in equilibrium when the total force exerted on it is zero; this occurs at the intersections of the lines and the force curve. For a given

stiffness, withdrawal of the AFM probe corresponds to displacements of the straight line to the right in the figure. As the line is displaced from left to right, it intersects the force curve first at one point, then at three points, and then at a single point again. Hence the system goes through three stages: a single-well dominated by the intermolecular potential, a double well, and then a single well dominated by the harmonic potential (Fig. 2). Thus a rupture, an abrupt jump from the bottom of one well to the bottom of the next well, is defined only for an intermediate range of cantilever positions. If the cantilever force is either sufficiently small or sufficiently large, no observable rupture takes place. When both wells are present, stochastic bond separation becomes possible. As the probe continues to be withdrawn, the first well disappears. The Hookean force exerted when this occurs is what we have defined as the critical rupture force. At the critical rupture force, the line representing the Hookean spring is tangent to the force curve. If the spring is sufficiently stiff, rupture will never be observed, as there will never be more than one intersection between the curve representing the intermolecular force and the line representing the cantilever force. For any given values of $k$ and $d$, the critical rupture force is given by solution to $k = -dF/dx$, where

$$F(x) = 12(V_0/x_0)\left[(x_0/x)^7 - (x_0/x)^{13}\right] \qquad (4)$$

is the intermolecular force. Fig. 4 shows the critical rupture force as function of $k$. The bond energy $V_0$

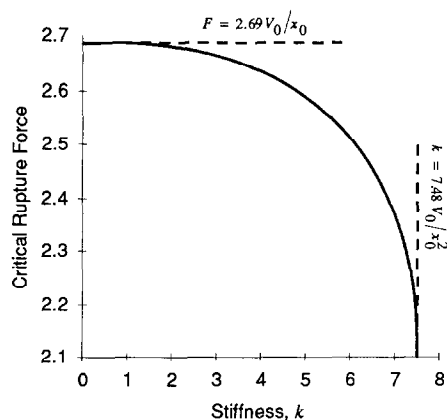

Fig. 4. Critical rupture force as a function of cantilever stiffness, $k$.

is equal to the work done in moving the ligand from $x_0$ to infinity in a potential field described by Eq. (3). Since the total work $W$ done by the AFM tip in rupturing the bond is equal to the area below the force curve, the total energy required to rupture the bond depends on the stiffness of the tip,

$$W = \int_{x_0}^{\tilde{x}} F(x)\,\mathrm{d}x$$

$$= V_0 - V_0 \left[ 2\left(\frac{x_0}{\tilde{x}}\right)^6 - \left(\frac{x_0}{\tilde{x}}\right)^{12} \right] \leq V_0 \qquad (5)$$

where $\tilde{x}\,(> x_0)$ is the intermolecular separation at the critical rupture force. Eq. (5) is interesting, since it says that it is not necessary for the tip to supply the entire bond energy $V_0 = \int_{x_0}^{\infty} F(x)\,\mathrm{d}x$ to separate the complex. The remaining bond energy is stored in the spring and is released in the rupturing process. Even more surprising is that for a system in solution, $W$ can be made small by selecting a sufficiently soft spring, i.e. one with $k$ very small.

For physiological measurements, the protein–ligand system is normally suspended in a viscous solution (e.g. water). This adds an additional term to the force (Eq. (4)),

$$F_{\text{viscous}} = \eta V \qquad (6)$$

where $\eta$ is the friction coefficient and $V$ the velocity. For a spherical particle of radius $r$, this is related to the viscosity $\xi$ (0.01 poise for water) as $\eta = 6\pi r \xi$ [19]. In the following calculations, the direct contribution of deterministic frictional forces to Eq. (4) has been neglected. However, viscosity does play a dominant role in describing the stochastic kinetics, as we shall see.

### 2.2. The rupture force measurements and their probability distribution

The microscopic motion of a macromolecule in a viscous solution undergoes rapid fluctuations due to its incessant collisions with the surrounding solvent molecules. Since the force involved in such Brownian motion is random, the dynamics of ligand dissociation from the molecular complex are described in terms of probabilities. When a bound ligand is subjected to an external potential, the probability distribution of the position $x$ and the velocity $V$ of the

ligand at time $t$, $P(x,V,t)$, can be obtained from a Fokker-Planck equation [20]. Kramers' rate theory [13] is based on the stationary solution of this one-dimensional differential equation with $E(x)$ exactly like the curves illustrated in Fig. 2. Applying Kramers' theory to chemical dynamics requires choosing an appropriate one-dimensional 'reaction coordinate'. Such a coordinate is provided naturally by the axis of the AFM probe, which makes our problem intrinsically one-dimensional, thereby removing one potential ambiguity from the analysis. One salient feature of Kramers' theory is the continuous passage from a high activation barrier, where Eyring's transition-state theory applies, to the low energy barrier where diffusion dominates. This is particularly important to the current analysis in which the energy barrier diminishes with increasing $d$.

Kramers solution makes the following assumptions: (i) near the bottom of the molecular well the complex is in equilibrium; (ii) at some point past the top of the barrier, escape is certain; (iii) there is no reverse reaction; and (iv) both the reactant well and the barrier may be approximated by quadratics in some small neighborhoods of the extrema. These assumptions can all be made for the one-dimensional AFM protein–ligand problem, which is then expressed as

$$B \overset{\kappa(d)}{\to} F \qquad (7)$$

where $B$ represents the 'bound' state of the protein–ligand pair and $F$ represents the 'free', or separated state. Since separated particles are collected and removed, the rate constant for the reverse reaction is zero (assumptions ii and iii). The probability distribution function, $P(t)$, that the protein–ligand complex is still bound at time $t$ is related to the rate constant as

$$\frac{\mathrm{d}P(t)}{\mathrm{d}t} = -\kappa(\mathrm{d}(t))P(t) \qquad (8)$$

Kramer's solution for the rate constant is

$$\kappa = \frac{\omega_R}{2\pi} e^{-E/\kappa T} \left\{ \sqrt{1 + (\eta/2m\omega_B)^2} - (\eta/2m\omega_B) \right\} \qquad (9)$$

where $\omega_R$ and $\omega_B$ are determined by the curvatures of the reactant well and activation barrier, respec-

tively. The effective spring constant is twice the coefficient of the quadratic term in a Taylor's series expansion of the $E(x)$; this is just the second derivative of the potential evaluated at the equilibrium. Hence

$$\omega_B = \sqrt{E''(x_B)/m} \tag{10}$$

and

$$\omega_R = \sqrt{E''(x_R)/m} \tag{11}$$

The rate constant can then be computed from Eq. (9) as described in the Section 3. Since the complex is initially bound,

$$P(t) = \exp\left\{-\int_0^t \kappa(d(\tau))d\tau\right\} \tag{12}$$

The probability that the complex is separated by time $t$ is $F(t) = 1 - P(t)$; the probability density function $f(t)$ for protein–ligand separation is the derivative of $F(t)$,

$$f(t) = \frac{dF}{dt} = \frac{d(1 - P(t))}{dt}$$

$$= \kappa(d(t))\exp\left\{-\int_0^t \kappa(d(\tau))d\tau\right\} \tag{13}$$

The mean and variance are $\mu = \langle t \rangle$ and $\sigma^2 = \langle t^2 \rangle - \mu^2$ where the brackets '$\langle \rangle$' denote average under the probability density function $f(t)$,

$$\langle t \rangle = \int_0^\infty t\kappa(d(t))\exp\left\{-\int_0^t \kappa(d(\tau))d\tau\right\}dt \tag{14}$$

$$\langle t^2 \rangle = \int_0^\infty t^2\kappa(d(t))\exp\left\{-\int_0^t \kappa(d(\tau))d\tau\right\}dt \tag{15}$$

These expressions are valid regardless of the motion of the probe. If the probe is withdrawn at a constant velocity, i.e. $d = x_0 + Vt$, then the probability density for rupture as a function of probe position $d$ is

$$p(d) = \frac{\kappa(d)}{V}\exp\left\{-\int_{x_0}^d \frac{\kappa(\rho)}{V}d\rho\right\} \tag{16}$$

When $V = 0$, Eq. (16) is undefined and the mean and variance must be computed from Eqs. (14) and (15). In this limiting case, the rate constant $\kappa$ is, in fact, a constant, and the probability density function
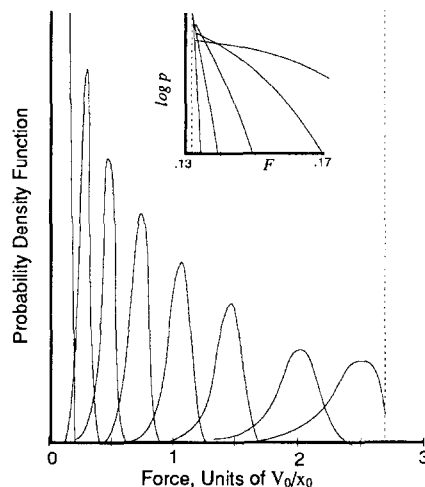


Fig. 5. Probability density function $f(\lambda)$ for protein–ligand separation at different cantilever speeds, normalized to give a total integral of 1 (the probability of protein–ligand separation by the time the AFM force is F is $\int_0^F f(\lambda)d\lambda$. Left to right, $V = 10^{-3}$ Å/s to $10^{11}$ Å/s in steps of 100 Å/s. Inset: low velocity limit, showing the approach to an exponential distribution, which would be linear on the semi-logarithmic plot. Left to right, $V = 3, 10, 30, 100, 300$ Å/μs. Parameters used for simulation: $x_0 = 2$ Å; viscosity = 0.01 poise (water); effective radius for friction = 5.3 Å; mass = 142 Daltons (e.g. biotin); well depth = 18.3 kcal/mol (e.g. for biotin–avidin); $T = 278.52$ K; $k = 61$ mN/m. The dashed vertical lines are at $F \approx 0.1319V_0/x_0$ (inset) and $F \approx 2.69V_0/x_0$.

becomes an exponential, $f(t) = \kappa e^{-\kappa t}$ with $\mu = \sigma = 1/\kappa$. Since the velocity is a continuous variable and the force is a continuous function of velocity and position, we expect the probability distribution as a function of force to approach an exponential distribution for very small withdrawal velocity (see Fig. 5 inset). The bond will eventually dissociate without pulling the probe if one is willing to wait long enough, and the time to dissociation is exponentially distributed. This is characteristic of a completely random (Poisson) process [21].

## 3. Method

The numerical implementation was as follows. The integral in Eq. (16) is set initially to zero and the cantilever is slowly withdrawn at a constant velocity $V$ starting at $x_0$ at $t = 0$. At each position of the cantilever, the reactant well location is determined

using Newton's method [22] for the roots of $dE/dx$ where $E(x)$ is given by Eq. (2). The first guess ignores the cantilever by setting $k = 0$ and the initial intermolecular separation to $x_0$. The position of the barrier is determined using a bisection algorithm because it is difficult to obtain a good first guess which will guarantee convergence with Newton's method. If there is no barrier, the cantilever is too close to the sample and the probability of escape is zero. If there is a barrier, the barrier and well frequencies can be obtained from Eqs. (10) and (11). The rate constant is then determined from Kramers' formula, Eq. (9), and the integral in Eq. (16) is updated using Euler's method [22] to give the probability density at $d$. The force applied by the tip of the AFM is calculated as $F = k(d - x)$ (see Fig. 1). The algorithm is then repeated iteratively until the probability density function is determined for an interesting range of $d$.

The entire procedure was then repeated for a wide range of velocities giving an ensemble of probability density functions, one function for each velocity. The mean and variance of the distributions were calculated and plotted as a function of velocity. All calculations were done in FORTRAN.

## 4. Results

The probability density functions (pdfs) for the force at which dissociation occurs are illustrated in Fig. 5 for a range of cantilever velocities. The mean and width of the distributions are shown in Fig. 6. The following observations are made:

1. As velocity increases, the distribution moves to the right. Since less time is spent in the low-force regime, by the time the probability of rupture becomes appreciably non-zero, higher forces are being applied to the protein–ligand system.

2. At lower velocities, the distribution widens with increasing velocity. If the probe is held at a fixed position, and the observer waits for a sufficiently long period of time, all of the protein–ligand pairs will eventually separate due to the stochastic forces (a zero-velocity extrapolation). Hence all pairs will separate (i.e. rupture) under the same applied force without variance. Hence the width of the distribution is zero. At slightly higher velocity, only a
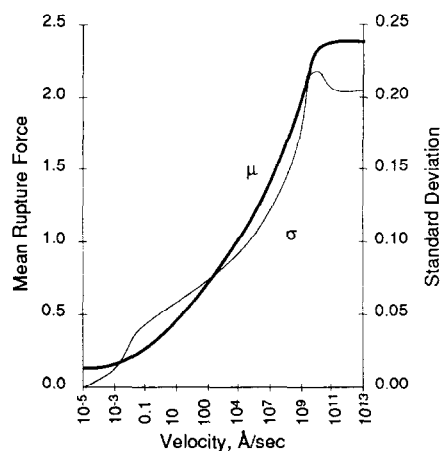


Fig. 6. Dependence of rupture force on cantilever velocity. $\mu$, $\sigma$ = mean, standard deviation of force, in units $V_0/x_0$, at protein–ligand separation.

finite amount of time is spent within any finite (small) range of forces, and hence the probability distribution will have a finite width.

3. The width of the distribution decreases at high velocity. When the probe is withdrawn very quickly, the potential function will very quickly pass through all three regimes: one-well, then two-well, then one-well again. The final transition from two-well to one-well is one of well coalescence, dominated by the critical rupture force. Well-coalescence is equivalent to rupture with a probability of one. The faster the probe, the sooner the third regime is reached, and less time is spent in the two-well, the stochastic regime. Hence the distribution width must decrease at high velocity.

4. There is a peak width to the distribution at an intermediate velocity; this follows immediately from the previous two observations and continuity.

5. There is a minimum force value, below which rupture is impossible and above which there is a finite possibility of rupture. This force corresponds to the minimum rupture force defined above at the one energy-well to two energy-well transition.

6. At high velocity, the probability of rupture is approximately Gaussian-shaped. At low velocity, the probability approaches an exponential distribution with a peak at the minimum rupture force. Rupture in this case is approaching a Poisson process with exponential distribution.
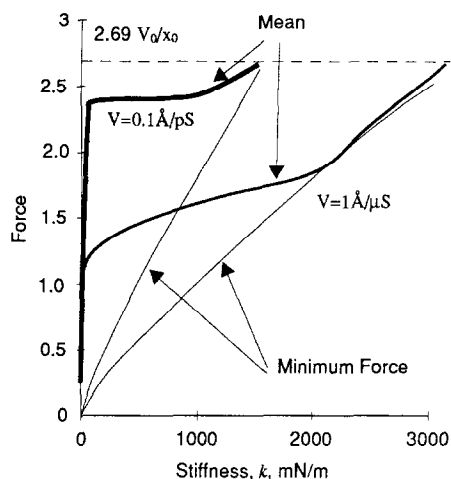
Fig. 7. Dependence of rupture force on harmonic constant, for two different velocities. Force is in units of $V_0 / x_0$. The two energy wells merge when the force reaches $\approx 2.69 V_0 / x_0$ (horizontal line in Fig. 4). The vertical asymptote in Fig. 4 (at $k \approx 7.48 V_0 / x_0^2$ or $F \approx 23.7$ N/m) is off scale to the right.

As we have discussed, the force necessary to separate the complex, which we have called the rupture force, is also a function of the spring constant of the cantilever. This is illustrated in Fig. 7. The minimum rupture force is a linear function of stiffness for the entire range of $k$ for which both potential wells in Fig. 2 exist. When the minimum rupture force reaches the critical classical value shown in Fig. 4, the two wells coalesce; for larger $k$-values, the rupture does not exist. This would correspond to the situation in Fig. 3 in which the line is so steep that it is never possible to intersect the force curve more than once regardless of the position of the cantilever.

## 5. Discussion

Our goal was to extract the core physical chemistry from the process of protein–ligand separation with the AFM; the resulting one-dimensional model provides a theoretical framework for real laboratory data analysis and produces quantitative results which are consistent with experimental measurements. For example, the avidin–biotin rupture force has been estimated at $160 \pm 20$ pN [9], from which we can estimate the order of magnitude for bond length.

From Fig. 4, $F \leq 2.69 V_0 / x_0$ hence $x_0 \leq 21$ Å (at $V_0 \approx 18.3$ kcal/mol and $k = 61$ mN/m, assuming the quoted value is the mean rupture force). The actual bond length (in this approximation) is somewhat less than this value, depending on the location of the knee in Fig. 4.

We have used Kramers' theory to study the protein–ligand dissociation under an external force. Our analysis assumes dissociation is a quasi-stationary process. Kramers' theory is known [23] to break down at either extremely high $(\eta \gg m\omega_B)$ or extremely low friction $(\eta \ll m\omega_B)$ due to the recombination of the protein–ligand pair. Both forms of breakdown are avoided in AFM experiments because the backward reaction does not occur.

Under normal experimental conditions multiple complexes will bind when the probe is brought into contact with the AFM substrate. The observed rupture statistics will thus have multiple peaks, corresponding to the number of bonds which are broken in a single observation, each of which is described by a probability density function (pdf) such as those illustrated in Fig. 5. The total observed histogram is then described by a weighted sum of the individual pdfs, where the weights give the probability of each number of complexes forming. The multiple-bond breaking can be characterized using a Poisson distribution (work in progress).

We have treated a single macromolecular complex in the simplest possible terms. In this model, the protein–ligand pair is represented as a compressible barbell with a simple 6–12 potential representing molecular interaction. One part of the complex is held fixed, while the other is pulled out by an external harmonic force (representing the AFM probe). This one-dimensional model ignores the true complexity of macromolecular interactions. In reality, these forces are not limited to a single dimension; multiple residues of the protein will usually bind to the ligand. Biotin, for example, interacts with at least eleven hydrophilic and five hydrophobic residues in avidin [24] and to at least seven residues of strepavidin [25]. Our model only considers the components of these bonds along the direction of the AFM axis, and lumps them all together into a single van der Waals' interaction, regardless of the geometry of the complex with respect to the apparatus. Hence $U(x)$ should be understood as a potential

describing the mean force between the protein and the ligand. In addition, while van der Waals' forces interacting with a particular site may dominate some configurations, there are usually other forces involved. To accurately describe single complex binding and rupture, one would expect that all of the these interactions must be taken into account [26]. However, care must be taken in these extrapolations to correctly interpret the results of a zero velocity extrapolation. With zero pulling speed, protein–ligand complex separation is essentially a Poisson process. The bond will eventually rupture stochastically subject to thermal forces (see result 2 and the discussion following Eq. (16) with the time to separation described by an exponential probability distribution [21].

## Acknowledgements

## References

[1] E. Neher, Ion channels for communication between and within cells, Science 256 (1992) 489–502.

[2] B. Sakmann, Elementary steps in synaptic transmission revealed by currents through single ion channels, Science 256 (1992) 503–512.

[3] E. Neher, C.F. Stevens, Conductance fluctuations and ionic pores in membranes, Annu. Rev. Biophys. Bioeng. 6 (1977) 345–381.

[4] E.L. Elson, H. Qian, The measurements of molecular transport in small systems, Lect. Math Life Sci. 24 (1994) 37–39.

[5] S.M. Block, Nanometers and piconewtons: the macromolecular mechanics of kinesin, Trends Cell Biol. 5 (1995) 169–175.

[6] S.C. Kuo, M.P. Sheetz, Force of single kinesin molecules measured with optical tweezers, Science 260 (1993) 232–234.

[7] E. Meyhofer, J. Howard, The force generated by a single kinesin molecule against an elastic load, Proc. Natl. Acad. Sci. USA 92 (1995) 574–578.

[8] S.B. Smith, L. Finzi, C. Bustamante, Direct mechanical measurement of the elasticity of single DNA molecules by using magnetic beads, Science 258 (1992) 1122–1126.

[9] E.L. Florin, V.T. Moy, H.E. Gaub, Adhesion between individual ligand receptor pairs, Science 264 (1994) 415–417.

[10] V.T. Moy, E-L. Florin, H.E. Gaub, Intermolecular forces and energies between ligands and receptors, Science 266 (1994) 257–259.

[11] G.U. Lee, L.A. Chrisey, R.J. Colton, Direct measurement of the forces between complementary strands of DNA, Science 266 (1994) 771–773.

[12] E.L. Florin, M. Rief, H. Lehmann, M. Ludwig, C. Dornmair, V.T. Moy, H.E. Gaub, Sensing specific molecular interactions with the atomic force microscope, Biosens. Biolectron. 10 (1995) 895–901.

[13] H.A. Kramers, Brownian motion in a field of force and the diffusion model of chemical reaction, Physica 7 (1940) 284–304.

[14] E. Evans, K. Ritchie, R. Merkel, Sensitive force technique to probe molecular adhesion and structural linkages at biological interfaces, Biophys. J. 68 (1995) 2580–2587.

[15] E. Evans, Dynamic force spectroscopy of weak adhesive bonds, Bull. Am. Phys. Soc. 41 (1996) 457.

[16] D. Sarid, Scanning Force Microscopy: With Applications to Electric, Magnetic, and Atomic Forces, Oxford University Press, New York, 1991.

[17] J.N. Israelachvili, Intermolecular and Surface Forces, 2nd ed., Academic Press, New York, 1991.

[18] A. Chilkoti, T. Boland, B.D. Ratner, P.S. Stayton, The relationship between ligand-binding thermodynamics and protein–ligand interaction forces measured by atomic force microscopy, Biophys. J. 69 (1995) 2125–2130.

[19] D. McQuarrie, Statistical Mechanics, Harper and Row, New York, 1976.

[20] S. Chandrasekhar, Stochastic problems in physics and astronomy, Rev. Mod. Phys. 15 (1943) 1–89.

[21] S. Karlin, H.M. Taylor, A First Course in Stochastic Processes, 2nd ed., Academic Press, New York, 1975.

[22] S.D. Conte, C. de Boor, Elementary Numerical Analysis: An Algorithmic Approach, 2nd ed., McGraw-Hill, New York, 1965.

[23] R.F. Grote, J.T. Hynes, The stable states picture of chemical reactions. II. Rate constants for condensed and gas phase reaction models, J. Chem. Phys. 73 (1980) 2715–2732.

[24] O. Livnah, E.A. Bayer, M. Wilchek, J.L. Sussman, Three-dimensional structures of avidin and the avidin–biotin complex, Proc. Natl. Acad. Sci. USA 90 (1993) 5076–5080.

[25] P.C. Weber, J.J. Wendolski, M.W. Pantoliano, F.R. Salemme, Crystallographic and thermodynamic comparison of natural and synthetic ligands bound to streptavidin, J. Am. Chem. Soc. 114 (1992) 3197–3200.

[26] H. Grubmüller, B. Heymann, P. Tavan, Ligand binding: molecular mechanics calculation of the streptavidin–biotin rupture force, Science 271 (1996) 997–999.